

---

# WPI

---

## **Investigation of Interaction of MIG-10 and ABI-1, Two Proteins Important for Neuronal Migration and Axon Guidance in *C. elegans***

---

Major Qualifying Project Report  
submitted to the Faculty of  
Worcester Polytechnic Institute  
in partial fulfillment of requirements for the  
Degree of Bachelor of Science  
Submitted by:

**Andrea Reis**

Submitted to:

---

Professor Elizabeth F. Ryder, Major Advisor

---

Professor Kristin Wobbe, Major Advisor

## **Abstract**

Cytoplasmic adaptor MIG-10 plays a role in neuronal migration and process outgrowth in *C. elegans*. Data from a yeast-two hybrid assay indicate that MIG-10 interacts with ABI-1, a protein involved in regulation of actin polymerization and required for neuronal migration and outgrowth. To further characterize the interaction between MIG-10 and ABI-1, deletion mutants were created and co-immunoprecipitation assays and western blots were performed. Preliminary results indicate that the C-terminal SH3 region of ABI-1 is required for its interaction with MIG-10.

## **Acknowledgements**

First I would like to thank Liz Ryder for guiding me through this project each step of the way, building my interest in neurobiology and other areas of biology, and helping me learn to be a better scientific reader and writer. I would like to thank Kris Wobbe for reminding me that there will always be obstacles in the laboratory and helping me problem solve and persevere. I would also like to thank Molly McShea for paving the way of this project goal before me, Karen Tran for answering my questions about co-immunoprecipitation and western assays, and Harita Menon for providing me with and helping me maintain cell cultures. I would also like to thank the Politz, Vidali and Duffy labs for sharing their knowledge and equipment. Last but not least, I would like to thank Meagan Sullender and Erin Maloney for helping teach me lab skills and keeping the laboratory fun and exciting.

## Table of Contents

<b>Table of Figures and Tables</b> .....	<b>5</b>
<b>Introduction</b> .....	<b>6</b>
Developmental Cell Migration and Axonal Outgrowth.....	6
<i>C. elegans</i> as a Model System .....	9
Mig-10 Structure and Function .....	10
MIG-10 Interacts with UNC-34.....	12
Axonal Outgrowth Signal Transduction Pathway Model .....	13
MIG-10 and ABI-1 Interaction .....	15
ABI-1 Structure and Function .....	16
Previous Research on MIG-10 and ABI-1 Interaction.....	18
Project Goals.....	20
<b>Materials and Methods</b> .....	<b>21</b>
Polymerase Chain Reaction.....	21
Gateway Cloning System .....	22
Cell Culture and Transfection .....	24
Co-Immunoprecipitation .....	24
Western Blotting .....	25
<b>Results</b> .....	<b>28</b>
Deletion Mutant Constructs.....	28
Protein Expression, Immunoprecipitation and Western Blotting.....	32
Transfection .....	33
Co-Immunoprecipitation and Western Blotting.....	34
<b>Discussion</b> .....	<b>39</b>
<b>References</b> .....	<b>43</b>

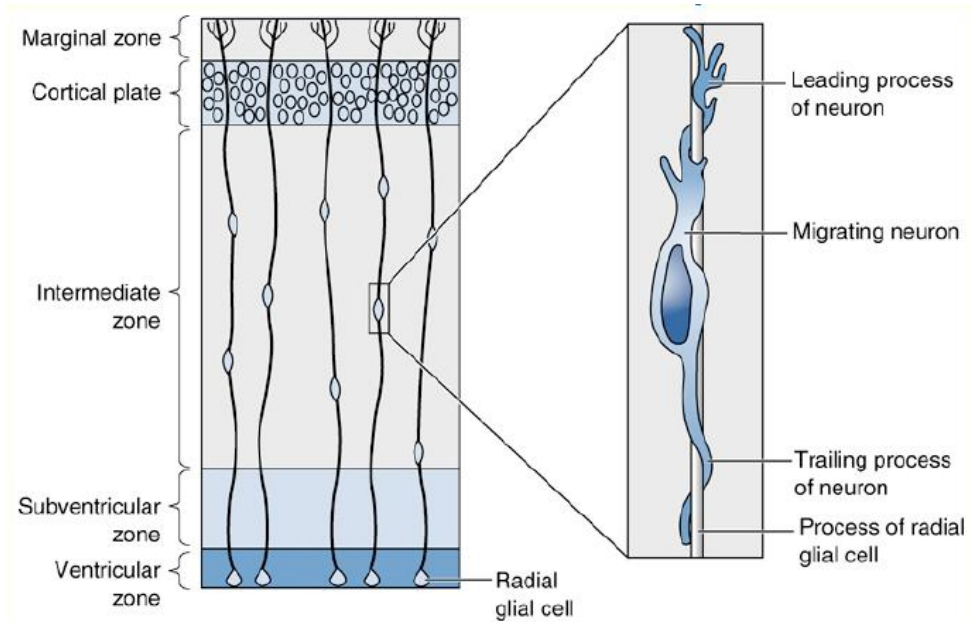
## Table of Figures and Tables

Figure 1: Neuronal Migration from the Ventricular Zone to the Cortical Plate. ....	7
Figure 2: Growth Cone. ....	8
Figure 3: ALM, CAN, and HSN Cell Migrations in <i>C. elegans</i> . ....	10
Figure 4: The Three Transcripts of Genomic <i>mig-10</i> . ....	11
Figure 5: The Three Protein Isoforms of MIG-10. ....	12
Figure 6: Current Model of Actin Remodeling with MIG-10. ....	15
Figure 7: ABI-1 Structure. ....	16
Figure 8: ABI-1 and MIG-10 Deletion Mutants. ....	18
Table 1: PCR Primers Used to Make the <i>abi-1</i> Deletion Mutant Constructs. ....	21
Figure 9: Gateway Cloning System. ....	23
Figure 10: ABI-1 Wild-type and Mutant Constructs. ....	29
Figure 11: Gel Electrophoresis of <i>abi-1(1-426)</i> and <i>abi-1(1-415)</i> Entry Clone Minipreps. ....	30
Figure 12: Gel Electrophoresis of <i>abi-1(416-469)</i> Entry Clone Minipreps. ....	31
Figure 13: Electrophoresis of <i>abi-1(1-415)::GFP</i> , <i>abi-1(1-426)::GFP</i> , and <i>abi-1(416-469)::GFP</i> Expression Clone Minipreps. ....	32
Figure 14: Overview of Assays Involved in Determining <i>in vitro</i> Protein Interaction. ....	33
Figure 15: Co-transfection of <i>abi-1::GFP</i> . ....	34
Figure 16: Western Blot of Mig-10 Variants Pulled Down With $\alpha$ -GFP and Probed for GFP and V5. ....	36
Figure 17: Western Blot of ABI-1(1-173)::GFP Pulled Down With $\alpha$ -GFP and Probed for GFP and V5. .	38

## Introduction

### Developmental Cell Migration and Axonal Outgrowth

During human development, billions of neurons form a complex network within the brain. Between the 5<sup>th</sup> week and 5<sup>th</sup> month of pregnancy, neurogenesis can reach a rate of 250,000 neurons formed per minute. Within the cortex of the brain, progenitor, or precursor cells develop in the ventricular zone of the telencephalic vesicle of the brain and give rise to neurons and glia. From the ventricular zone cells migrate out towards the pia mater, a thin membrane near the surface of the brain, to form the six layers of the cortex. To begin this process, the cell extends a process out toward the pia and the cell nucleus moves toward the surface of the pia. There the DNA inside the nucleus is replicated. The nucleus, with two copies of the DNA, migrates back down into the ventricular zone. Lastly the cell retracts the process from the pia and the cell divides in two, producing daughter cells. Early in development, the two daughter cells stay in the ventricular zone and each continues the proliferation process. Later on in development, however, one of the daughter cells migrates into the cortex to form part of an upper cortical layer (Figure 1). This migration is very organized, with an inside-out mechanism in which the outermost cortical layer (VI) forms first, followed by layer V, etc.



**Figure 1: Neuronal Migration from the Ventricular Zone to the Cortical Plate.** During early development, neuroblasts migrate along radial glial processes from the ventricular zone towards the cortical plate. Within the cortical plate, the neurons form six layers by an inside-out mechanism in which the first set of migrated neurons form the innermost layer (Bear *et. al*, 2007).

The cell migration process is directed by radial glial cells. Daughter cells move along paths provided by radial glial cells from the ventricular zone to their destinations in the cortical layers. Once a cell reaches its final destination, it undergoes differentiation and forms connections to other cells that provide the nerve network in our brain. After differentiation occurs, cells are no longer able to divide. Differentiated neurons produce growth cones that develop into axons and dendrites (Figure 2). Growth cones include lamellipodia which are membranes on the tip of the cone that contain spiky filopodia, acting as legs to extend the growth cone (Bear *et. al*, 2007).

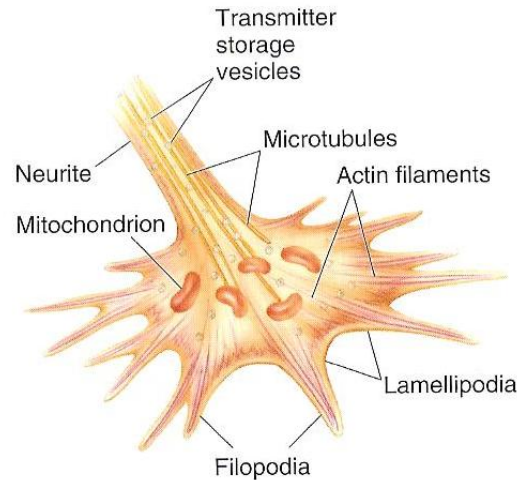


**Figure 2: Growth Cone.** Lamellipodia extend out from the axon as filopodia respond to guidance cues. (Bear *et. al*, 2007).

Guidance cues are required to direct the growth cones to extend in a specific direction.

Guidance cues can be attractive, guiding the axon towards it, or repulsive, pushing the axon away in an opposing direction. To direct the growth, guidance cues cause polarization of the growth cone by the accumulation of F-actin and microtubules on one side of the growth cone tip (Quinn and Wadsworth, 2008).

Improper cell migration and axonal outgrowth during brain development causes disorders associated with mental retardation. One such disorder is corpus callosum dysgenesis. In patients with corpus callosum dysgenesis axons fail to make a connection between the left and right hemispheres. The connection can be partially or completely missing, causing mild to severe mental retardation (Engle, 2010). Studying the normal process of cell migration and axonal outgrowth is the first step to determining what causes the improper migration and extensions of cells. After the cell migration process is further understood, the underlying causes of corpus callosum dysgenesis and similar disorders can be studied. This could one day lead to the creation of treatments and neuroregenerative therapies to ameliorate or eliminate the symptoms of neuronal migration disorders.

This project aimed to improve our understanding of the developmental cell migration process in the model system *C. elegans* by characterizing interaction between two proteins, MIG-10 and ABI-1, known to be involved in cell migration and process outgrowth. The interactions between different domains of each protein were studied *in vitro* to determine which domains of MIG-10 and of ABI-1 are required for their interaction. Mutations affecting the interacting domains of either protein could disrupt the cell migration process and therefore may be a contributing factor in neuronal migration disorders. This project furthered our knowledge of the domains of MIG-10 and ABI-1 required for the two proteins' interaction, thus indicating potential areas where mutations could cause disruption in the cell migration process.

### ***C. elegans* as a Model System**

While guidance cues of axonal outgrowth have been well-studied, mechanisms that link guidance cues and the polarization of cell processes are not fully understood. One useful model system in which the cell migration process is more easily studied is the nematode species *Caenorhabditis elegans*. *C. elegans* has a much simpler nervous system than humans and other vertebrates, consisting of only 302 neurons (Brenner, 1974). *C. elegans* are also transparent, making *in vivo* studies of the worms easier with fluorescent tagging of cells (Chalfie, 1994).

In *C. elegans*, the excretory cell and neurons, such as the HSN, ALM, and CAN, are useful in studying cell migration and process outgrowth. During development, the excretory cell body forms ventrally near the pharynx and extends multiple processes or canals dorsolaterally almost the length of the whole nematode. These processes then divide and extend anterior and posterior through *C. elegans* (Buechner, 2002). *C. elegans* embryos also have several neurons that undergo long-range migrations during development. These neurons, including HSN, ALM, and CAN, are easily visible under a microscope (Figure 3; Hedgecock *et al.*, 1987). MIG-10 is one protein known to be involved in the cell migration

process of *C. elegans*. A null allele of the *mig-10* gene, *mig-10(ct41)*, resulted in truncation of the excretory canals and shortened migrations of the cell bodies of the HSN, AVM and CAN (Manser and Wood, 1990).

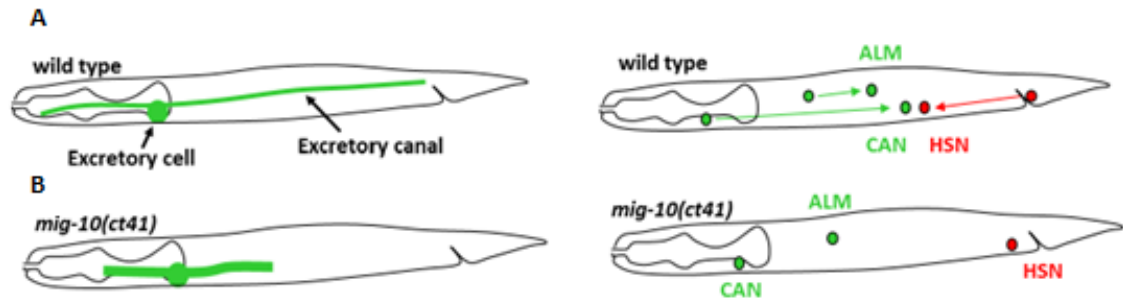


**Figure 3: ALM, CAN, and HSN Cell Migrations in *C. elegans*.** **A:** Wild-type *mig-10* in *C. elegans*; highlights the length of the wild-type excretory canal and migrations of the ALM, CAN, and HSN neurons. **B:** *mig-10(ct41)*, a null allele of *mig-10* in *C. elegans*; the excretory canal is truncated compared to the wild-type and migrations of the ALM, CAN, and HSN are shortened (McShea, 2011).

### MIG-10 Structure and Function

MIG-10 is a *C. elegans* ortholog of the vertebrate proteins RIAM and lamellipodin. This family acts as cytoplasmic adaptor proteins which are involved in signal transduction processes (Lafuente *et. al*, 2004; Krause *et. al*, 2004). MIG-10 expresses three transcripts which encode three isoforms, MIG-10A, MIG-10B and MIG-10C (Manser *et. al*, 1997; Figures 4 and 5). Each isoform contains a Ras-association domain (RA), pleckstrin homology domain (PH), and EVH1 binding sites (FP4) near the N and C termini. The RA domain is known to bind to CED-10/Rac-GTP complexes and the PH domain is known to bind to phosphatidylinositol (3,4) bisphosphate in the cell membrane (Quinn *et. al*, 2008). Data are consistent with the hypothesis that one or both of the FP4 regions of MIG-10 bind to UNC-34/Ena/VASP (Quinn, *et. al*, 2006; Chang *et. al*, 2006). The three isoforms only differ at the N termini, in length and sequence.

To determine which isoforms of MIG-10 are sufficient for excretory canal outgrowth, fosmids (bacterial F-plasmids) expressing *mig-10a* and *mig-10b* transcripts were tested for their ability to rescue

excretory cell canal truncation in *mig-10(ct41)* mutants *in vivo*. Fosmids expressing both *mig-10a* and *mig-10b*, but not *mig-10c*, transcripts displayed wild-type excretory canals in *mig-10(ct41)* mutants, indicating that *mig-10c* is not required for excretory canal outgrowth (Zhang, 2010; McShea, 2011). To test whether MIG-10 functions cell autonomously in the excretory cell, *mig-10a* or *mig-10b* cDNA was expressed specifically in the excretory cell. Both isoforms rescued excretory canal defects and no significant difference was found between excretory canal lengths in the presence of the MIG-10A or MIG-10B isoforms. These results show that MIG-10A or MIG-10B isoforms are sufficient for excretory cell outgrowth when expressed cell autonomously in the excretory cell.

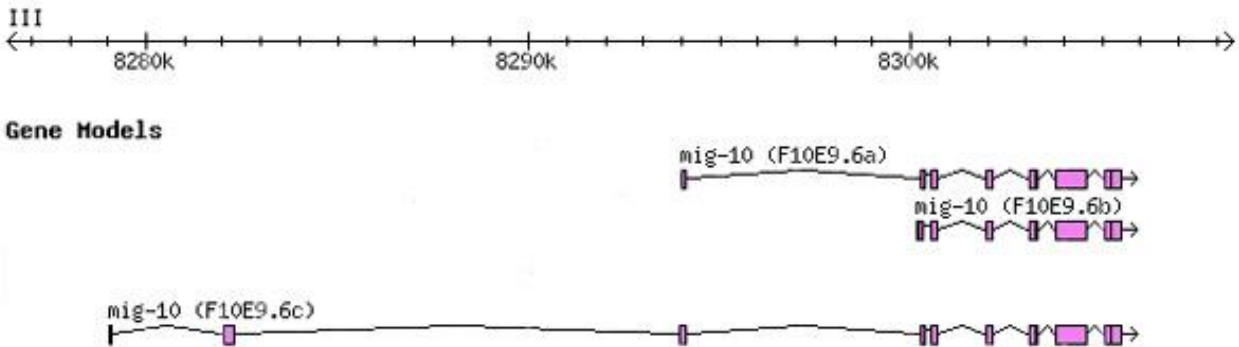


**Figure 4: The Three Transcripts of Genomic *mig-10* (Wormbase).** Each transcript differs in the length and sequence of the 5' exons. The middle regions and 3' exons are identical in both length and sequence of all three transcripts. Each transcript also has different upstream sequences which may act as promoters and therefore each transcript may be differentially regulated. *mig-10c* is denoted as (F10E9.6c) and has the longest N-terminus; it has not been shown to play a role in the cell migration process. *mig-10a* is denoted as (F10E9.6a) and *mig-10b* is denoted as (F10E9.6b). *mig-10a* is the main transcript which has been studied for protein interaction with *abi-1* and is the transcript used in this project.

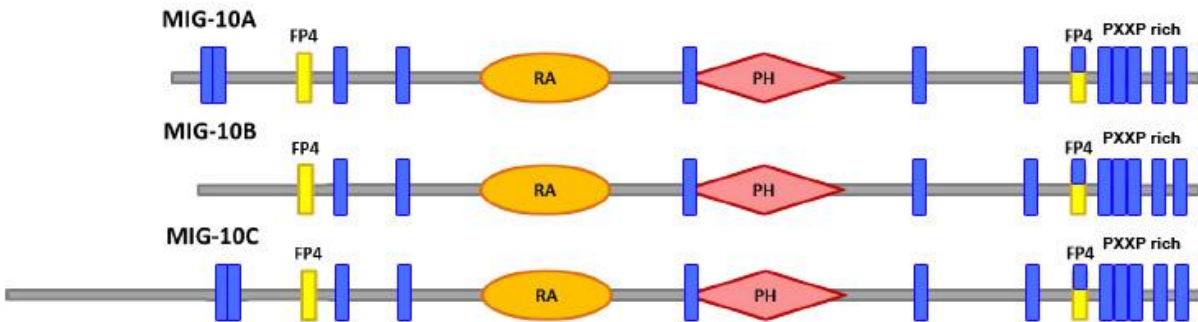


**Figure 5: The Three Protein Isoforms of MIG-10.** The C terminus FP4 regions (yellow), Ras-association domain (RA) (orange) and Pleckstrin homology domain (PH) (red) are identical in the MIG-10A, MIG-10B, and MIG-10C isoforms. The RA and PH domains bind to CED-10/Rac-GTP and phosphatidylinositol (3,4) bisphosphate, respectively, during the cell migration process. The two FP4 regions with consensus sequence: (D/E)(F/L/W/Y)PPPPX(D/E)(D/E), are EVH1 binding sites, that putatively bind to UNC-34/Ena/VASP. 13 PXXP regions are potential SH3 binding sites (blue) (Manser *et al*, 1997; Figure modified from McShea, 2011).

## MIG-10 Interacts with UNC-34

UNC-34 is the only member of the Ena/VASP family of proteins found in *C. elegans*. The EVH1 domains of the Ena/VASP family of proteins bind to proline-rich EVH1 binding sites of MIG-10/Lamellipodin, causing co-localization of UNC-34 with MIG-10 to the growth cone. Ena/VASP helps promote elongation of actin by bundling, prevention of G-actin capping of the barbed ends of F-actin, and debranching. Experiments with null *unc-34* mutants resulted in a significant decrease in the number of filopodia in HSN growth cones (Chang *et. al*, 2006). Overexpression of UNC-34 however led to approximately triple the number of filopodia observed in the HSN neurons of the wild-type. Another experiment was conducted in which the null *mig-10(ct41)* mutant was expressed in addition to UNC-34 overexpression. This resulted in suppression of the overexpressed UNC-34 phenotype. Combined, these results suggest that UNC-34 is required for the growth of filopodia and that MIG-10 is required upstream of UNC-34 (Chang *et. al*, 2006).

## Axonal Outgrowth Signal Transduction Pathway Model

The current model of axonal outgrowth (Figure 6) involves MIG-10 localization to the cell membrane as an integral step. Overall, in response to guidance cues, CED-10/Rac-1 is activated, causing localization of MIG-10/Lamellipodin which then binds to UNC-34, resulting in regulated growth of the filopodia. This project focuses on creating a better understanding of how ABI-1 interacts with MIG-10 during this process.

During axon guidance, MIG-10 functions downstream from UNC-6/Netrin and SLT-1/Slit guidance cues (Quinn et al., 2006). UNC-6 serves as an attractive guidance cue for axonal outgrowth, secreted from the ventral side of the worm, while SLT-1 is a repellant guidance cue, secreted from the dorsal side. Both guidance cues cause the AVM axon in *C. elegans* to move towards the ventral nerve cord. When MIG-10 is overexpressed in the absence of both guidance cues (*slt-1; unc-6* double mutants), axonal outgrowth still occurs. However, the result is often a multipolar neuron in which the outgrowth appears less directed. When either guidance cue was wild-type, axonal outgrowth was rescued back to monopolarity. Furthermore, overexpression of MIG-10 with guidance cues causes enhancement of the axonal growth toward the ventral nerve cord (Quinn et al., 2006; Chang et al., 2006). Adler also observed localization of MIG-10 to the ventral plasma membrane of the HSN neuron (Adler et al., 2006). These results suggest that guidance cues lead to the localization of MIG-10 to a certain area of the cell to accomplish monopolar outgrowth of an axon.

The current model is consistent with data indicating that MIG-10/Lamellipodin is localized through binding of its central RAPH (Ras-association and pleckstrin homology domains) region to activated CED-10/Rac-1. CED-10/Rac-1 is a G protein, activated by exchange of its GDP for GTP. *In vitro* binding assays were conducted in which MIG-10-RAPH::GFP binding to CED-10/Rac-1 was shown to be GTP dependent (Quinn et al., 2008). This result indicates that MIG-10 will only bind to activated CED-

10/Rac-1. Activated CED-10/Rac-1 is required for the localization of MIG-10, which stimulates directed, monopolar outgrowth of the axon. CED-10 is likely to be activated locally by the presence of a guidance cue. Further studies found that the MIG-10 binding to Rac-GTP was conserved in lamellipodin but not in the RIAM ortholog (Quinn *et. al*, 2008).

The next step in axonal outgrowth in *C. elegans* is the binding of UNC-34 to MIG-10. Specifically, the first 118 amino acids of MIG-10A, containing a putative EVH1 binding site, have been shown to interact with UNC-34 (Quinn *et. al*, 2006). Likewise, MIG-10A amino acids 458-651, containing another putative EVH1 binding site, may also bind UNC-34 (Chang *et. al*, 2006). The current model, consistent with these data, suggests that one or both of the putative EVH1 binding sites (designated FP4) of localized MIG-10 bind to the EVH1 domain of UNC-34 protein. The model then indicates that UNC-34 promotes the elongation of actin through debranching, anticapping and bundling. However, null *unc-34* mutants resulted in a less severe phenotype than that of null *mig-10(ct41)* mutants. This difference in phenotypic severity between null mutants suggests that MIG-10 may also be interacting with another protein that regulates actin elongation (Quinn, *et. al*, 2006).

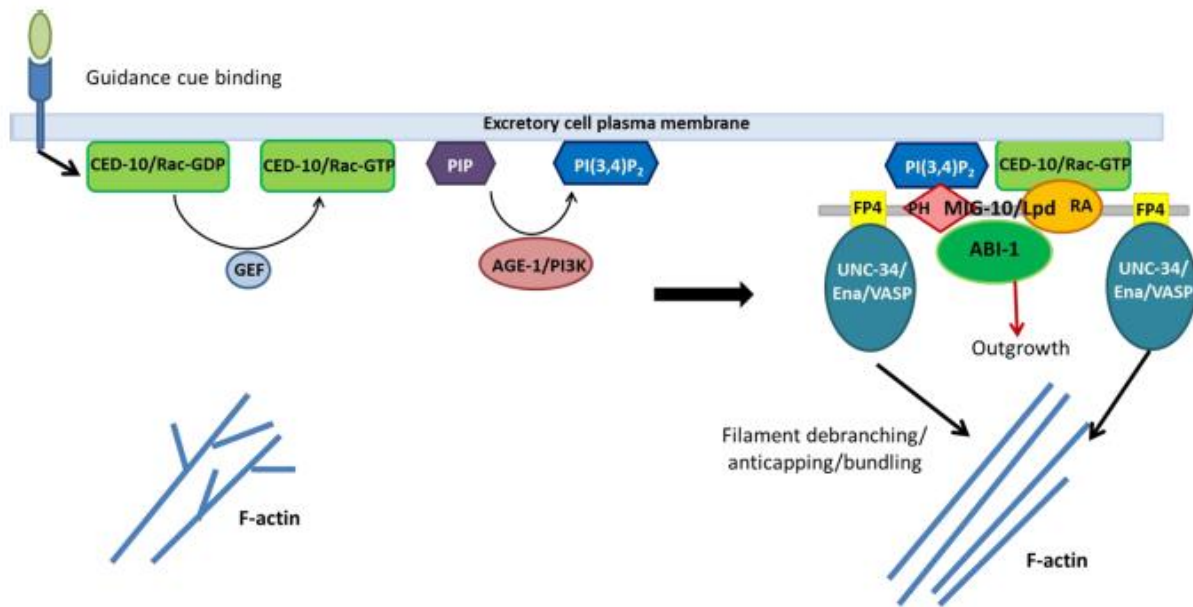


**Figure 6: Current Model of Actin Remodeling with MIG-10.** A guidance cue signal contacts the cell and stimulates an exchange of GDP for GTP in the CED-10/Rac-GDP complex by a guanine nucleotide exchange factor (GEF) and phosphorylation of phosphatidylinositol phosphate (PIP) to phosphatidylinositol (3,4) bisphosphate (PI(3,4)P<sub>2</sub>). These activated molecules recruit MIG-10 to the plasma membrane, binding the PH domain of MIG-10 to PI(3,4)P<sub>2</sub> and the RA domain of MIG-10 to the CED-10/Rac-GTP complex. MIG-10 localization to the plasma membrane recruits UNC-34 to the cell membrane via the FP4 regions of MIG-10. UNC-34 activity leads to elongation of F-actin in the direction of the guidance cue. ABI-1 is believed to bind to a region of MIG-10 and play a role in the cytoskeletal remodeling (McShea, 2011).

## MIG-10 and ABI-1 Interaction

In order to explore the idea that MIG-10 may interact with another protein during the axonal outgrowth process, Gosselin and O'Toole (2008) conducted a yeast-two hybrid analysis. The yeast-two hybrid analysis involved using one of the MIG-10 isoforms, MIG-10A, to screen a *C. elegans* cDNA library for any proteins that can have interactions with MIG-10. The study found that ABI-1 was the strongest candidate for interaction with MIG-10 because it was isolated in six separate transformations of the cDNA library. The present study focuses on determining the domains of each protein required for interaction between MIG-10 and ABI-1, which are thought to be involved in actin remodeling during cell migration and axonal outgrowth in *C. elegans*.

## ABI-1 Structure and Function

Abelson-interactor-1, or ABI-1, is a protein found in *C. elegans* downstream of Abelson tyrosine kinase (Abl). Vertebrates often have three Abi family members, similar to ABI-1 of *C. elegans*. The ABI family is involved in the binding of actin and regulation of actin dynamics (Echarri *et. al*, 2004). Near the N terminus ABI-1 contains a Q-SNARE domain next to an ABL-HHR domain (Schmidt *et. al*, 2009; Figure 7). A wave-binding domain (WAB) which binds to the actin nucleator protein WAVE-1 is also located near the N terminus. A serine rich domain is in the middle of the protein. Several putative Src-homology 3 (SH3) binding domains are toward the C terminus with an SH3 domain on the C terminus. One function of the SH3 domain is to bind to proline-rich regions of other proteins. The SH3 domain may be involved in interaction with MIG-10, since MIG-10 has several proline-rich regions (McShea, 2011). Thus, one goal of this project was to create deletion mutant constructs of ABI-1 to determine if the SH3 domain of ABI-1 is required and sufficient for interaction with MIG-10. However, ABI-1 is known to be involved in several cellular processes from WAVE and Rac activation to Mena phosphorylation. Several of these processes could also be related to the function of ABI-1 and MIG-10 interaction.

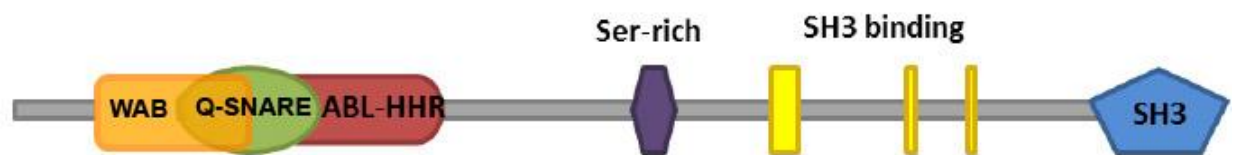


**Figure 7: ABI-1 Structure.** ABI-1 has a Wave Binding Domain (WAB) which overlaps with the Q-SNARE domain near the N terminus. The Q-SNARE domain is followed by an ABL-HHR domain, a serine-rich middle region, SH3 binding sites and an SH3 domain on the C terminus. The SNARE domain is conserved in mammals and is required for binding to Syntaxin-1. The SH3 domain binds to proline-rich regions of other proteins and is thought to be involved in interaction with MIG-10 (modified from McShea, 2011).

One process that ABI-1 is involved in is Rac activation. Rac is a GTPase protein that is involved in actin remodeling. To activate Ras to Rac, a GEF (Sos-1) exchanges a GDP for a GTP. This exchange takes place when a multi-protein complex forms between the GEF, ABI-1 and an actin barbed-end capping

protein, EPS8. Abi-1 association with EPS8 activates EPS8 which regulates the GEF activity and thus Rac activation. The EPS8/ABI-1 complex may also be involved in actin polymerization and other actin-related processes (Disanza *et. al*, 2005).

ABI-1 also activates WAVE, an interactor of Arp2/3 complex. Arp2/3 is a protein complex which branches actin filaments. ARP2/3 complex alone cannot polymerize actin branching. Nucleation Promoting Factors (NPFs) such as the WASP and WAVE families activate the Arp2/3 complex. These NPFs relay signals from Cdc42 and Rac to the Arp2/3 complex. The NPFs are regulated through different processes. Inactivation of WAVE1 occurs through the formation of a complex with proteins Nap-1 and PIR121-Sra-1. WAVE2 is believed to be positively regulated by ABI-1. ABI-1 binds directly to WAVE2 forming a WAVE-ABI1-Nap1-PIR121 complex which increases WAVE-mediated actin polymerization. Thus ABI-1 plays a regulatory role in WAVE-mediated actin polymerization (Disanza *et. al*, 2005).

ABI-1 is also involved in some phosphorylation processes such as phosphorylation of the protein Mena. ABI-1 was determined to be an interactor with Mammalian Enabled (Mena), through a yeast-two hybrid system. Binding assays found that the proline rich domain of ABI-1 and the Ena/VASP homology 1 domain of Mena interact. ABI-1 promotes the tyrosine phosphorylation of Mena by c-Abl. It is suggested that ABI-1 regulates this phosphorylation by interacting with both Mena and c-Abl (Tani *et. al*, 2003). Lamellipodin, the vertebrate homolog of MIG-10, is also phosphorylated by Abl (Michael *et. al*, 2010). ABI-1 could interact with MIG-10 and/or UNC-34 similarly to its role in the Mena/c-Abl phosphorylation.

Overall, ABI-1 localizes to the tips of lamellipodia and filopodia. In vertebrates, when the interaction between ABI-1 and WAVE-1 is interrupted, ABI-1 does not localize to the lamellipodia tips (Echarri *et. al*, 2004). In *C. elegans*, *abi-1* mutants were used to study its function in the cells. *abi-1(tm494)* is a hypomorphic, or loss of function, allele of *abi-1*. In mutants homozygous for *abi-1(tm494)*,

the excretory canals were truncated, similar to the *mig-10(ct41)* mutants (Schmidt, *et. al*, 2009). In addition, *abi-1(RNAi)* greatly enhanced the truncation of the excretory canal observed in *mig-10* mutants (Dubuke and Grant, 2009). *abi-1(tm494)* mutants also have defects in neuronal migration (McShea *et. al*, unpublished results). This evidence suggests that ABI-1 and MIG-10 have similar roles in the cell migration and outgrowth processes (McShea, 2011).

### Previous Research on MIG-10 and ABI-1 Interaction

ABI-1 and MIG-10 both function *in vivo* in the excretory cell of *C. elegans*. McShea (2011) used a co-immunoprecipitation assay in *D. melanogaster* cells for further analysis of their interaction. V5 tags were used for MIG-10 and MIG-10 deletion mutants. GFP tags were used for ABI-1 and ABI-1 deletion mutants. The different deletion mutants analyzed are shown in Figure 8 below.

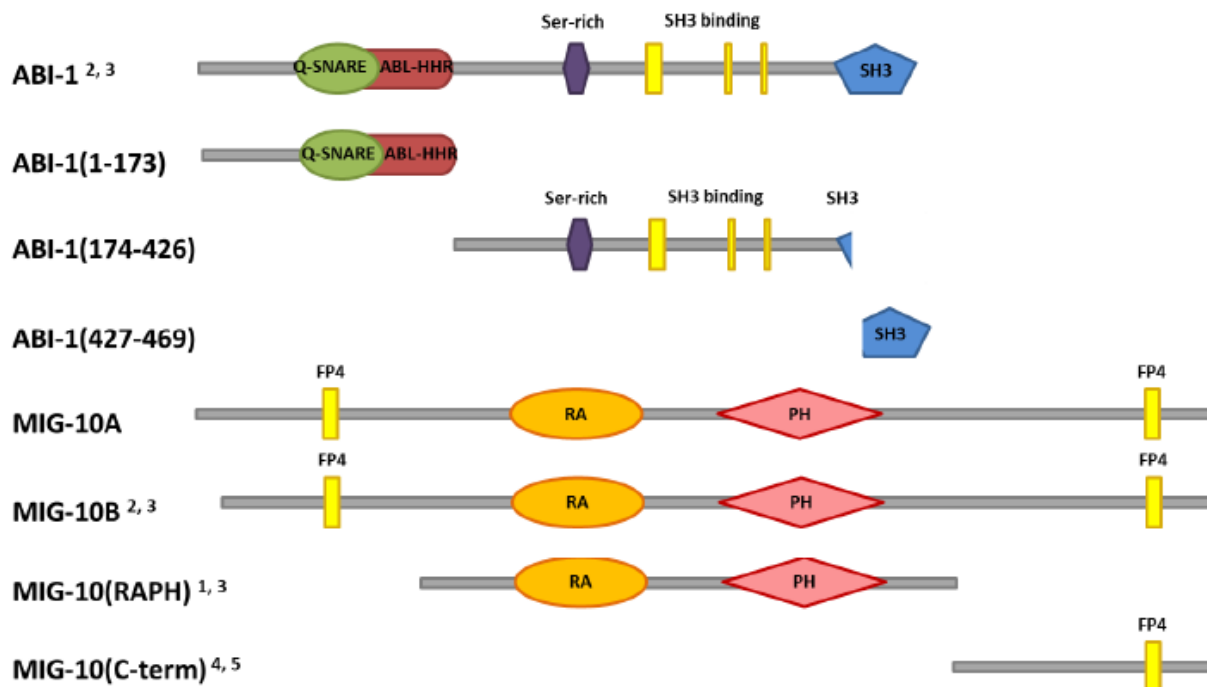


**Figure 8: ABI-1 and MIG-10 Deletion Mutants.** Wild-type and mutant ABI-1 proteins were fused with GFP tags on the C terminus and wild-type and mutant MIG-10 proteins were fused with V5 tags on the C terminus. Wild-type and mutant proteins were analyzed for interaction using co-immunoprecipitation and Western blotting using anti-V5 antibodies (McShea, 2011).

Repeated co-immunoprecipitation of wild-type MIG-10A::V5 and mutant ABI-1(174-426)::GFP (missing the N terminus and most of the SH3 domain), followed by western blotting with anti-V5 antibody resulted in minimal isolation of MIG-10A::V5, while wild-type MIG-10A::V5 and ABI-1::GFP showed higher levels of isolation, indicating first that co-immunoprecipitation of MIG-10A::V5 is specific to wild-type ABI-1::GFP (McShea, 2011). Furthermore, the N-terminus and/or the SH3 domain of ABI-1 are required to mediate the interaction with MIG-10A. McShea then conducted co-immunoprecipitation of various deletion mutant constructs of both proteins. Preliminary results of western blots, using anti-V5 antibody, showed that wild-type ABI-1::GFP and ABI-1(427-469)::GFP, containing most of the SH3 region, were both able to co-immunoprecipitate MIG-10A::V5, MIG-10(RAPH)::V5, and MIG-10(C-term)::V5. MIG-10 variants were not visibly isolated when co-expressed with the N terminus of ABI-1 (ABI-1(1-173)::GFP). These preliminary results suggest that only the SH3 domain is required for interaction with MIG-10, however, these results were not able to be repeated.

Since the yeast two hybrid and other experiments only focused on MIG-10A, MIG-10B was also tested for interaction with ABI-1. Co-immunoprecipitation of MIG-10B::V5 and ABI-1::GFP with western blotting using anti-V5 antibody resulted in isolation of MIG-10B::V5, indicating that MIG-10B can also interact with ABI-1 and therefore ABI-1 is not isoform specific to MIG-10. Since MIG-10A and MIG-10B differ in their N termini it is not likely that the N-termini interact with ABI-1 (McShea, 2011).

Overall, preliminary results have indicated that the SH3 domain of ABI-1 and the RAPH and C-term domains of MIG-10 are involved in the interaction of the two proteins. Based on these results, this project attempted to gather more data on the co-immunoprecipitation of ABI-1 and MIG-10 wild-type and deletion mutant proteins.

## Project Goals

The goal of this project was to further characterize the interaction of MIG-10 and ABI-1 in the cell migration process. Specifically, the domains of ABI-1 and MIG-10 that are required for their interaction were studied. To accomplish this goal, ABI-1 and MIG-10 wild-type and deletion mutant proteins with fluorescent tags were studied *in vitro*. Based on McShea's results, it appears that the SH3 domain of ABI-1 may be required for the interaction between the two proteins. To further support this hypothesis, new *abi-1* constructs were made using the Gateway Cloning System. Two constructs were created in which only the SH3 domain is missing (*abi-1(1-415)::GFP* and *abi-1(1-426)::GFP*) and one construct was made in which only the SH3 domain is present (*abi-1(416-469)::GFP*). It was expected that interaction with MIG-10 would only be seen when the ABI-1 SH3 domain was present; however, the new constructs were not available in time for use in this project. Next, previous co-immunoprecipitation experiments by McShea were repeated in order to confirm interaction or lack of interaction between the wild-type and mutant proteins. Western blotting was used to detect the fluorescent tags and determine whether the 2<sup>nd</sup> protein was able to interact with the 1<sup>st</sup> protein. The results of this project will help further the understanding of the role of MIG-10 and ABI-1 in the cell migration process in *C. elegans*, which could lead to a better understanding of the homologs involved in the cell migration process of human development.

## Materials and Methods

### Polymerase Chain Reaction

PCR was conducted with 0.5 Units of Vent polymerase (New England Biolabs), 1X Thermopol buffer (New England Biolabs), 200  $\mu$ M dNTPs, 0.4  $\mu$ M of forward and reverse primers (Table 1), and approximately 4 ng of the wildtype template, per 25  $\mu$ L reaction. PCR was run with an initial denaturing step at 94°C for 5 minutes followed by 35 cycles consisting of: 94°C denaturing for 30 seconds, 57°C annealing for 1 minute, and 72°C extension for 1 minute. 5  $\mu$ L of each sample was run on a 0.8% agarose gel in 1X TAE buffer to determine if the PCR product was the approximate size expected. Once the PCR product was confirmed on the gel, the DNA was then used without further purification in the Gateway Cloning System.

**Table 1: PCR Primers Used to Make the *abi-1* Deletion Mutant Constructs.** Three new *abi-1* deletion mutant constructs, *abi-1(1-415)*, *abi-1(1-426)*, and *abi-1(416-469)* were created using the primers below.

Construct Name	Forward Primer	Forward Primer Sequence	Reverse Primer	Reverse Primer Sequence
ABI-1(1-426)	Abi_foratt	5" GGG GAC AAC TTT GTA CAA AAA AGT TGG AAA ATG AGT GTT AAT GAT CTT CAA GAG 3"	Abi-1-174-426_R	5" GGG GAC AAC TTT GTA CAA GAA AGT TGG TGC AGC ATC ATA GTC GTA CAG G 3"
ABI-1(1-415)	Abi-1-N_foratt	5" GGG GAC AAC TTT GTA CAA AAA AGT TGG AAA ATG AGT GTT AAT GAT CTT CAA GAG CTC ATC 3"	Abi-1-415_revatt	5" GGG GAC AAC TTT GTA CAA GAA AGT TGG TTC CAA ATA CTC GTT GGG CAT CCA TCC AGC AC 3"
ABI-1(416-469)	Abi-416_foratt	5" GGG GAC AAC TTT GTA CAA AAA AGT TGG AAA ATG AAA GTA CGG GTC CTG TAC GAC TAT G 3"	Abi_revatt	5" GGG GAC AAC TTT GTA CAA GAA AGT TGG TAC TGG AAC TAC GTA GTT TCC AG 3"

## Gateway Cloning System

Using the Gateway Cloning System (Figure 9), 2 to 5.5  $\mu\text{L}$  of PCR product, for approximately 150 ng, was put into the BP reaction with 1.5  $\mu\text{L}$  of pDONR vector for approximately 150 ng, 1  $\mu\text{L}$  TE buffer, and 2  $\mu\text{L}$  BP Clonase II enzyme (Invitrogen). The reaction proceeded overnight at 25°C. 5  $\mu\text{L}$  of the resulting clone was then transformed into 50  $\mu\text{L}$  of Max-Efficiency DH5 $\alpha$  *E. coli* competent cells (Invitrogen) by incubating on ice for 30 minutes, then heat shocking the cells at 42°C for 30 seconds and adding 400  $\mu\text{L}$  of SOC (Invitrogen). The transformation was incubated on a nutator at 37°C for one to three hours. Cells were then plated on LB plates containing 50  $\mu\text{g}/\text{mL}$  Kanamycin and allowed to grow overnight at 37°C. Individual colonies on each plate were isolated and placed in 5 mL aliquots of LB with 50  $\mu\text{g}/\text{mL}$  Kanamycin. The QIAprep Spin Miniprep kit from Qiagen was then used to perform minipreps for each sample. 2 to 3  $\mu\text{L}$  of each sample were removed for a restriction digest. 1  $\mu\text{L}$  of restriction enzymes such as HindIII, BamHI, or BanII (New England Biolabs) with 1X BSA (New England Biolabs) as appropriate, 2  $\mu\text{L}$  of corresponding 10X buffer (New England Biolabs), 2  $\mu\text{L}$  of the sample DNA, and appropriate amount of dH<sub>2</sub>O, were combined for the 20  $\mu\text{L}$  sample digest and incubated at 37°C for two hours. After the restriction digest, samples were placed in a 0.8% agarose gel and run for approximately 1 hour at 100 V. 10  $\mu\text{L}$  of approximately 50 ng/ $\mu\text{L}$  DNA samples were sent to Genewiz for sequencing, following Genewiz recommendations.

Once the proper sequence was confirmed, 2 to 5.5  $\mu\text{L}$  of sample, for approximately 150 ng, was put into the LR reaction. The LR reaction and subsequent DNA purification and sequencing were performed as detailed for the BP reaction with a few exceptions. The LR reaction required 150 ng of pUAST-GFP destination vector and 2  $\mu\text{L}$  LR Clonase II enzyme (Invitrogen). High Efficiency DH5 $\alpha$  *E. coli* chemically competent cells (New England Biolabs) were used. During the transformation, after heat-shocking, cells were placed on ice for 5 minutes and then 950  $\mu\text{L}$  of SOC was added. The transformation

was incubated on a nutator at 37°C for one hour. Cells were grown using Ampicillin selection (50 ug /ml) instead of Kanamycin.

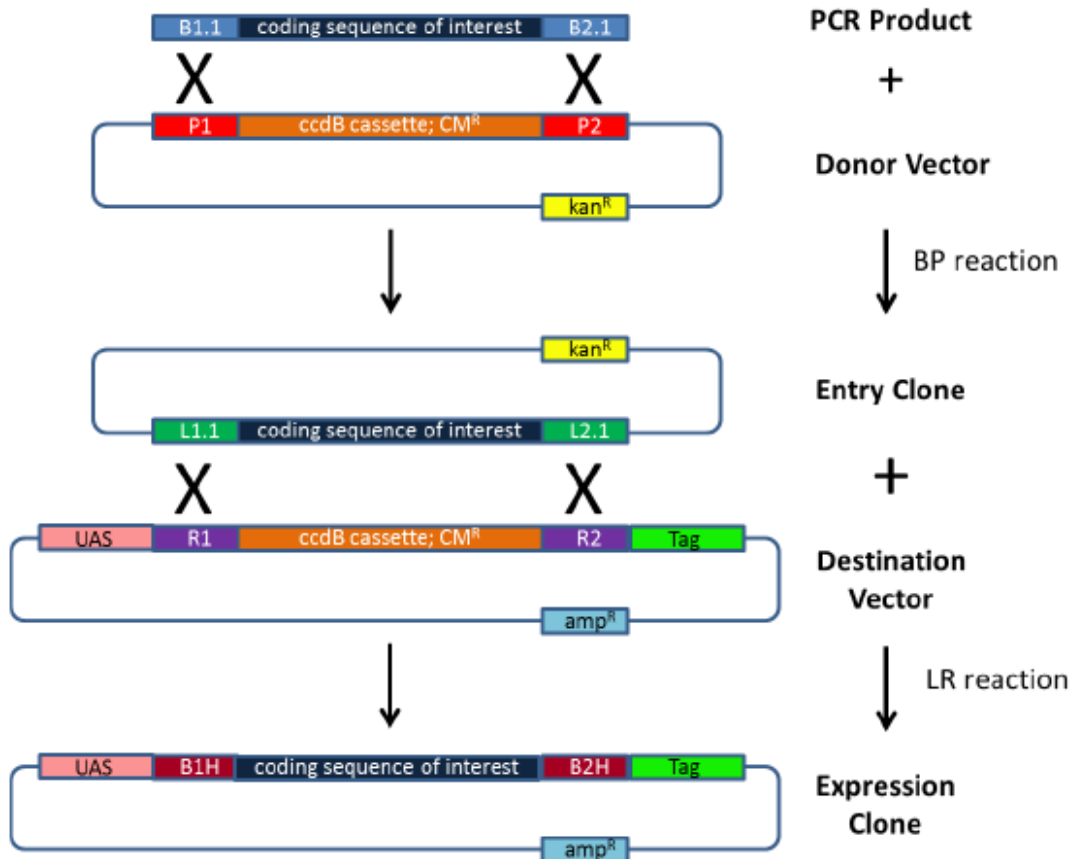


**Figure 9: Gateway Cloning System (Invitrogen).** First, wild-type or mutant PCR product with attB1.1 and attB2.2 sites and Donor Vector with attP1 and attP2 sites were mixed in solution. Recombination between the two sites was catalyzed by BP Clonase II to form an entry clone with the desired sequence. Recombination of the attB and attP sites formed attL sites in the entry clone. The second step used LR Clonase II to catalyze recombination between the entry clone attL1.1 and attL2.1 sites and the Destination Vector attR1 and attR2 sites, producing an expression clone with B1H and B2H sites, the desired coding sequence and a V5 or GFP tag (McShea, 2011).

## Cell Culture and Transfection

*S3 Drosophila melanogaster* cells were used to express the wild-type and mutant proteins. *S3* cells were fed 1X Schneider's media (Gibco) with 12.5% FBS (Valley Biomedical) by volume and split 1:10 every 3-4 days. Two days after a split, cells were diluted 1:10 with media. 2.0 mL of the diluted cells were placed into separate wells in a 6 well plate. After three more days, when cells were approximately 80-95% confluent, transfection was started. Protein construct concentrations were diluted to 66.6 ng/ $\mu$ L with TE buffer. Arm::GAL4 was also diluted to 66.6 ng/ $\mu$ L with TE buffer. Using sterile technique in the tissue culture hood, old media was removed from each well and 2.0 mL of 1X PBS was added and allowed to sit for approximately 30 seconds. The PBS was removed and 1.6 mL of new media was placed in each well. 96  $\mu$ L of EC buffer (Qiagen) was added to sterilized Eppendorf tubes. 2.0  $\mu$ L of each expression construct and 2.0 to 4.0  $\mu$ L of arm::GAL4 were added to individual tubes. 3.2  $\mu$ L of Enhancer (Qiagen) was added to each tube, stirred, and incubated for 2-5 minutes. Then 10  $\mu$ L of Effectene (Qiagen) was added to each tube, stirred gently, and incubated for 5-10 minutes. 600  $\mu$ L of new media was then added to each tube. The solutions were then added to individual wells. Cells were harvested 3-5 days after transfection.

## Co-Immunoprecipitation

Cells from each co-transfection were resuspended in their existing media and 200  $\mu$ L were removed for whole cell lysate (WCL) samples. The WCLs were centrifuged at approximately 4000 x g (or 8000 rpm in a micro-centrifuge) for 5 minutes and the supernatant was removed. Pellets were resuspended in 100  $\mu$ L of 1X Sample Buffer (12 mM Tris-HCl, pH 6.8; 5% glycerol; 0.4% SDS; 2.88 mM  $\beta$ -mercaptoethanol; 0.02% bromophenol blue) and stored at 4°C overnight. The remainder of each co-transfection was transferred to a 15 mL conical and centrifuged at 560 x g (or 2000 rpm) for 2 minutes at

4°C. The supernatant was removed and cells were lysed in 1 mL of Lysis buffer (containing 2X protease inhibitor (Roche) and 1X phosphatase inhibitor (1 mM sodium orthovanadate, 5 mM sodium pyrophosphate, 5 mM sodium fluoride) in EBC buffer (50 mM Tris, pH 8, 150 mM NaCl, 2 mM EDTA, 0.5% NP-40)). The cells were vortexed until resuspended and incubated on ice for 15 minutes. After incubation, cell debris was pelleted by centrifugation at approximately 16,500 x g (or 14,000 rpm in a table-top centrifuge) for 10 minutes at 4°C. The supernatants were then transferred to new tubes and 1 µL of mouse monoclonal anti-V5 antibody (Invitrogen) or 2 µL of rabbit polyclonal anti-GFP antibody (Clontech) were added to each sample. Samples were incubated on a nutator at 4°C for 30 minutes to 2 hours. After incubation, if monoclonal anti-V5 antibody was used, 50 µL of Protein A magnetic beads (Miltenyi Biotec) were added or 100 µL were added if polyclonal anti-GFP antibody was used. Samples were incubated at 4°C for a minimum of 30 minutes.

Magnetic columns (Miltenyi Biotec) were placed on a magnetic board and Eppendorf tubes were placed underneath to collect waste. Columns were rinsed with 200 µL of Lysis buffer. Cell lysates were then loaded onto the column. 200 µL of Lysis buffer was washed through the columns four times. Columns were then rinsed with 100 µL of Buffer X (50 mM Tris, pH 8.5, 250 mM NaCl, 2 mM EDTA and 1% NP-40) followed by 100 µL of Final Wash Buffer (50mM Tris, pH 8). New collection tubes were placed under the columns and 20 µL of 2X Sample Buffer (preheated to 95°C for 5 minutes) was added to each column and incubated for 5 minutes. An additional 50 µL of 2X sample buffer was added to each column and co-immunoprecipitates were stored at -20°C overnight.

## **Western Blotting**

10% resolving gels were prepared using 2.09 mL dH<sub>2</sub>O, 1.67 mL Solution A (29.2% acrylamide, 0.8% bis-acrylamide), 1.25 mL Solution B (1.5 M Tris-HCl, pH 8.8, 0.4% SDS, 21% (v/v) dH<sub>2</sub>O). 25 µL 10% APS and 2.5 µL TEMED were added just before pouring for a total of approximately 5 mL per gel. The

resolving gel was poured between two glass plates in a BioRad western apparatus and topped with ethyl alcohol to prevent evaporation. Once the resolving gel polymerized, the ethyl alcohol was removed and the stacking gel: 1.15 mL dH<sub>2</sub>O, 0.33 mL Solution A, 0.5 mL Solution C (0.5 M Tris-HCl, pH 6.8, 0.4% SDS and 46% (v/v) dH<sub>2</sub>O) with 15 µL 10% APS and 2.5 µL of TEMED added just before pouring) was poured on top of the resolving gel. Once the stacking gel polymerized, the whole gel (with its plates) was immersed in 1X electrophoresis buffer and the wells were rinsed with buffer. Co-immunoprecipitates and WCLs were boiled at 100 °C for 5 minutes before loading onto the gels. 5 µL of EZ-Run Pre-stained Rec Protein Ladder (Fisher) or Novex Sharp Pre-Stained Protein Standard (Invitrogen) and 10 µL of each sample were loaded into individual wells. Gels were run at 20 mA for approximately 2-3 hours.

A nitrocellulose/ECL membrane (GE Healthcare) and the transfer apparatus containing fiber pads and Whatman paper were prepared by soaking in 1X transfer buffer for approximately 15 minutes. The gel was then removed from the gel plates, the stacking gel was removed and the resolving gel was soaked in transfer buffer for 5 minutes. The gel was placed inside the transfer apparatus, on top of a fiber pad and Whatman paper, and then the membrane was laid over it with another Whatman paper and fiber pad on top. The protein transfer was run at 100V for 1 hour.

After the transfer, a Pierce West Pico SuperSignal Kit was used to immunoblot the protein. The membrane was blocked in approximately 20 mL of 5% non-fat dry milk (NFDM) in TBST (20 mM Tris, pH 7.6; 150 mM NaCl; 0.1% Tween-20) for 30-60 minutes and then rinsed in TBST. The membrane was incubated overnight at 4°C with primary antibody diluted with 10 mL of TBST in 1% NFDM for anti-V5 antibody or 0.5% NFDM for anti-GFP antibody. Primary antibody was 1:5,000 diluted mouse monoclonal anti-V5 antibody (Invitrogen) for V5-tagged proteins or 1:1,000 mouse monoclonal anti-GFP antibody (Clontech) for GFP-tagged proteins. After incubation, the membrane was washed with approximately 20 mL of TBST for 5 minutes, 5 times and then incubated with 1:40,000 diluted secondary antibody: HRP

conjugated goat anti-mouse antibody (Jackson ImmunoResearch Labs) for 1 hour at room temperature. The membrane was washed with approximately 20 mL of TBST for 5 minutes, 5 times and then placed on plastic wrap and covered with 1.5 mL substrate working solution (1:1 peroxide:luminol). The membrane was then placed in a sheet protector in an autoradiography cassette to transfer to a darkroom. Under red light, a piece of film was exposed to the membrane for an amount of time ranging from 30 seconds to 5 minutes. The film was then developed using a Kodak X-omat.

## Results

The main goal of this project was to determine which regions of ABI-1 are required for interaction with MIG-10. To achieve this goal several different methods were used. First, deletion mutant constructs of *abi-1* were made using PCR and the Gateway Cloning System. The second step involved co-transfection and co-immunoprecipitation assays between different ABI-1 and MIG-10A constructs to allow for possible *in vitro* interaction of the proteins and deletion mutant constructs. Lastly, western blots were performed to detect if interaction occurred between two proteins.

### Deletion Mutant Constructs

Several deletion mutant variants of MIG-10 and ABI-1 were previously created using the Gateway Cloning System. These variants include MIG-10(RAPH)::V5, MIG-10(C-term)::V5, ABI-1(1-173)::GFP, ABI-1(174-426)::GFP, and ABI-1(427-269)::GFP (Figure 8). Previous preliminary data are consistent with the model that the SH3 region of ABI-1 is required for interaction with MIG-10. Therefore this project aimed to make three new ABI-1 deletion mutant proteins (Figure 10). The first additional deletion mutant, ABI-1(1-415)::GFP would be used to determine if the SH3 domain is required for interaction with MIG-10 through lack of interaction without the SH3 domain. The second additional mutant, ABI-1: ABI-1(1-426)::GFP, contains a small portion of the SH3 domain and was made to be consistent with earlier experiments in which a slightly different boundary for the SH3 domain was defined. The third new deletion mutant construct containing only the SH3 region, ABI-1(416-469)::GFP, would be used to determine if the SH3 domain is sufficient for interaction with MIG-10.

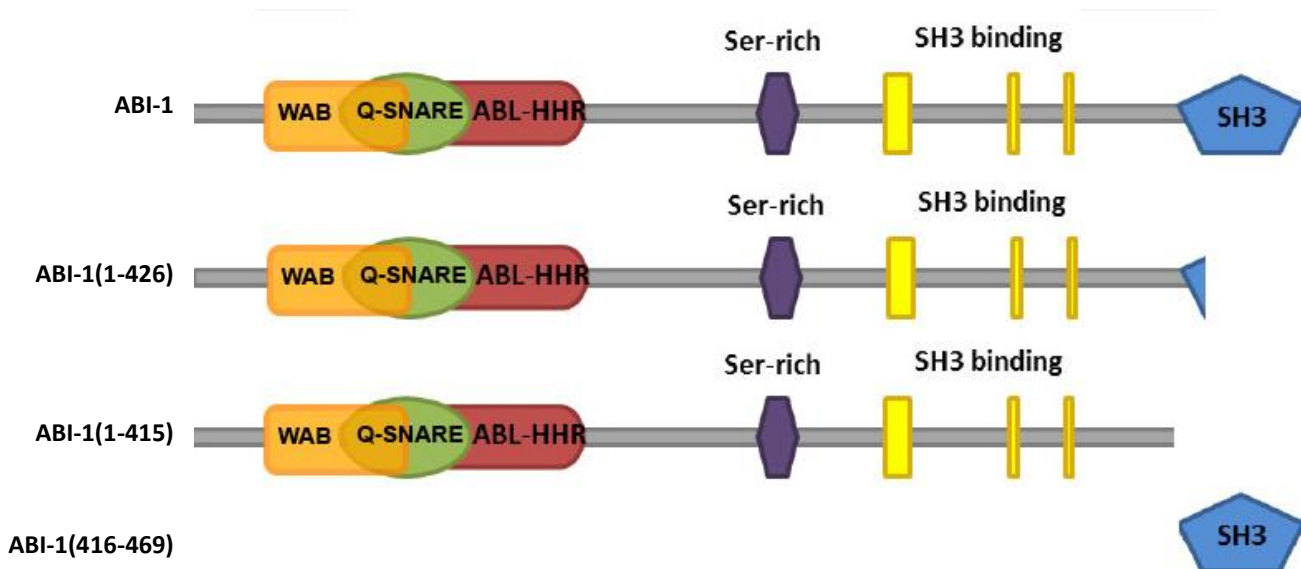
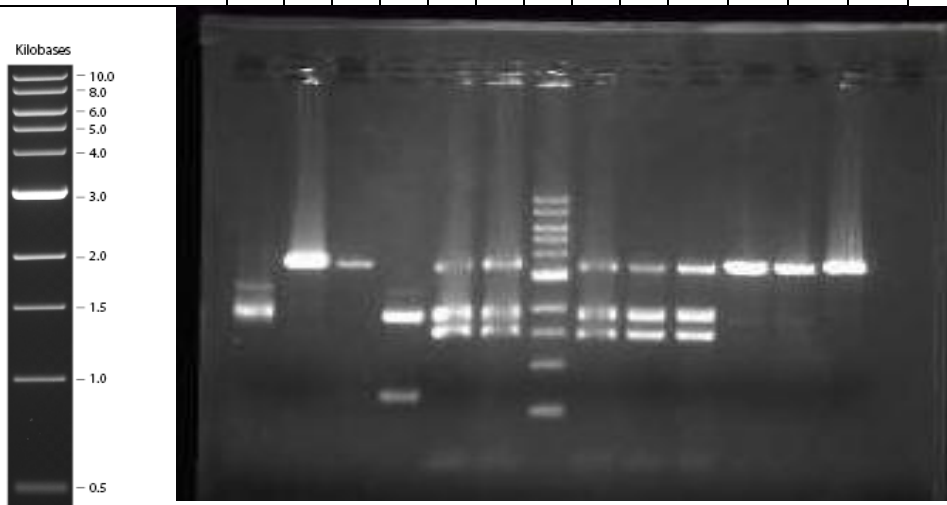


**Figure 10: ABI-1 Wild-type and Mutant Constructs.** The full length wild-type *abi-1* construct is shown at the top. *abi-1* mutants were created missing a portion of the SH3 region (ABI-1(1-426)), missing the whole SH3 region (ABI-1(1-415)), and only containing the SH3 region (ABI-1(416-470)). These mutants were made using PCR and the Gateway Cloning System.

Creation of the new deletion mutant constructs began by PCR of ABI-1 with forward and reverse primers corresponding to respective ABI-1 sequences (Table 1). PCR products were confirmed by samples run on a 0.8% agarose gel. Each PCR product was recombined with a donor vector (containing the Kanamycin resistance gene) with BP Clonase II in the BP reaction of the Gateway Cloning System. The resulting entry clone was transformed into 50  $\mu$ L of Max-Efficiency DH5 $\alpha$  *E. coli* competent cells and then selected for by plating on LB plates containing 50  $\mu$ g/mL Kanamycin. Individual colonies were grown up in 5 mL aliquots of LB with 50  $\mu$ g/mL of Kanamycin. Minipreps were performed for each sample. Samples were then digested with different restriction enzymes and confirmed with a 0.8% agarose gel with 1kb DNA ladder (NEB) (Figures 11 and 12). The expected lengths of bands of *abi-1*(1-426) with digestion by HindIII was 3732 bp and with digestion by BanII were 1851, 1623, 227 and 31 bp. Clone 1 did not show matching lengths and was not used further. Clones 3 and 5 show bands of the expected lengths. The expected lengths of bands of *abi-1*(1-415) with digestion by HindIII was 3699 bp

and with digestion by BanII were 1851, 1590, 227 and 31 bp. Clones 1, 3, and 5 showed bands of expected lengths.

Construct	<i>abi-1(1-426)</i>						L A D D E R	<i>abi-1(1-415)</i>					
	HindIII			BanII				BanII			HindIII		
Clone	1	3	5	1	3	5		1	3	5	1	3	5
Lane	1	2	3	4	5	6	7	8	9	10	11	12	13

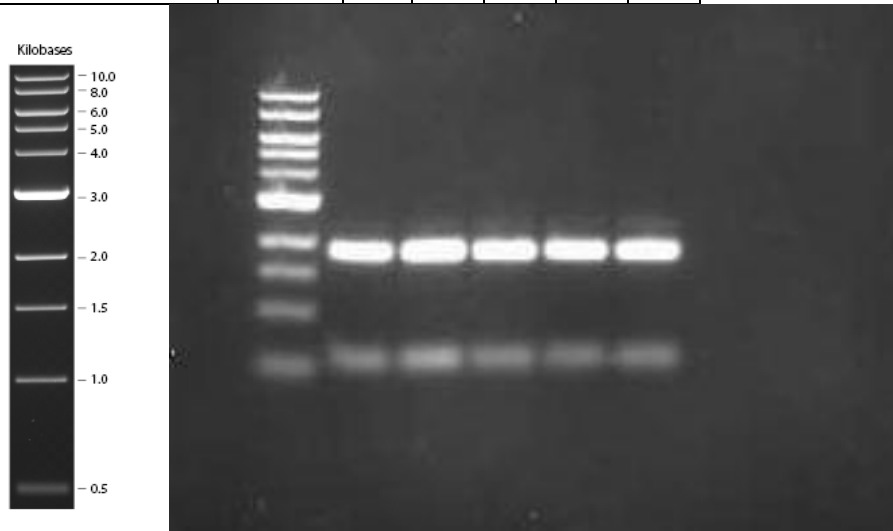


Ladder legend

**Figure 11: Gel Electrophoresis of *abi-1(1-426)* and *abi-1(1-415)* Entry Clone Minipreps.** A restriction digest of clones 1, 3, and 5 of each construct was performed individually with HindIII and with BanII restriction enzymes. *abi-1(1-426)* clones 3 and 5 and *abi-1(1-415)* clones 1, 3, and 5 were confirmed.

The expected lengths of bands of *abi-1(416-469)* with digestion by BanII were 1851 and 766 bp. Clones 1-5 showed bands of expected lengths. The sequences of the appropriate clones were then confirmed by Genewiz.

Construct		<i>abi-1(416-469)</i>				
Restriction Enzyme	LADDER	BanII				
Clone		1	2	3	4	5
Lane	1	2	3	4	5	6

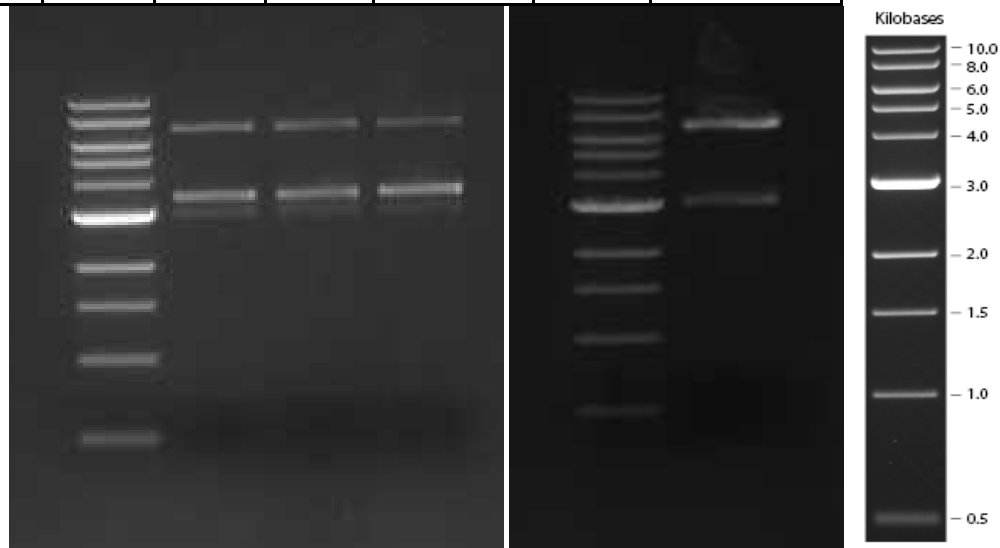


Ladder legend

**Figure 12: Gel Electrophoresis of *abi-1(416-469)* Entry Clone Minipreps.** A restriction digest of clones 1-5 was performed with BanII. All five *abi-1(416-469)* were confirmed.

Sequenced entry clones were recombined with GFP destination vector, pUASTaceGFP, (with an Ampicillin resistance gene) in the LR reaction with LR Clonase II. The resulting expression clones were then transformed and selected for by plating on LB plates containing 50 µg/mL Ampicillin. Individual colonies were grown up in 25-50 µg/mL Ampicillin and minipreps were performed. The resulting clones were digested with HindIII and run on a 0.8% agarose gel. Gel electrophoresis showed partial digests for each construct (Figure 13). Expected band lengths were 7285, 2993, 743, 44 and 24 bp for *abi-1(1-415)::GFP*, 7318, 2993, 743, 44 and 24 bp for *abi-1(1-426)::GFP*, and 6946, 2993, 44 and 24 bp for *abi-1(416-469)::GFP*. Bands seen between 3-4 kb for each clone are partial digests in which HindIII did not cut at all restriction sites. Each clone was sent out to Genewiz for sequencing and sequences were confirmed.

Construct	L A D D E R	<i>abi-1</i> (1-415)::GFP		<i>abi-1</i> (1-426)::GFP	L A D D E R	<i>abi-1</i> (416-469)::GFP
Restriction Enzyme		HindIII				HindIII
Clone		1	2	1		1
Lane	1	2	3	4	5	6



Ladder legend

**Figure 13: Electrophoresis of *abi-1*(1-415)::GFP, *abi-1*(1-426)::GFP, and *abi-1*(416-469)::GFP Expression Clone Minipreps.** Clones were digested with HindIII and run on a 0.8% agarose gel. Each clone was only partially digested, however all clones were confirmed by sequencing.

## Protein Expression, Immunoprecipitation and Western Blotting

In order to determine if there is interaction between ABI-1 and MIG-10 variants a series of assays involving protein expression, immunoprecipitation and western blotting were used (Figure 14). Wild-type and mutant constructs were co-transfected into an insect system. Arm::GAL4, which binds to an upstream activating sequence (UAS) upstream of the cloned gene fusions, was used to promote to the expression of the desired genes. Immunoprecipitation by anti-GFP antibody was then used to pull down the ABI-1::GFP variants. If interaction occurred between an ABI-1::GFP variant and a MIG-10::V5 variant (co-transfected in the same well) then the MIG-10::V5 variant should be co-immunoprecipitated with the ABI-1::GFP variant. Anti-GFP antibody was used during western blotting to show presence of

ABI-1::GFP brought down, while anti-V5 antibody was used to show presence, if interaction occurred, of MIG-10::V5 variants brought down. This system, with co-immunoprecipitation and whole cell lysate controls, allowed for further clarification of the domains of MIG-10 and ABI-1 involved in their interaction.

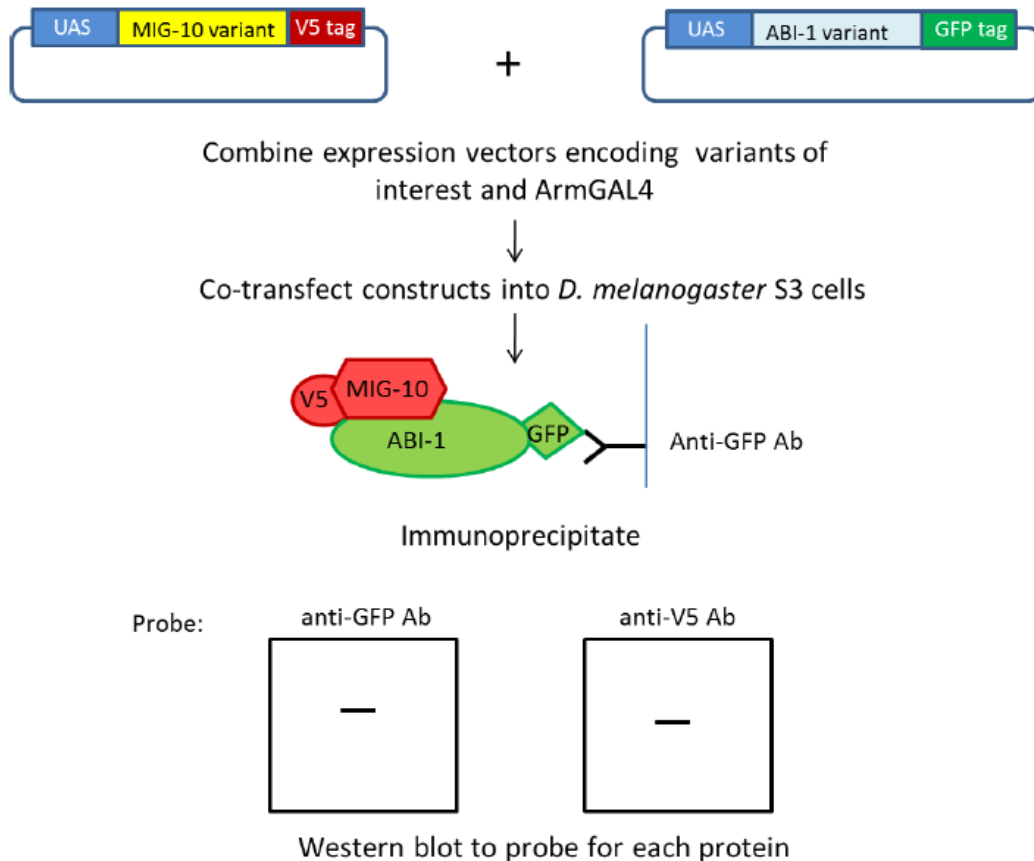


**Figure 14: Overview of Assays Involved in Determining *in vitro* Protein Interaction.** Co-transfection with Arm::GAL4 was used to express *abi-1* and *mig-10* constructs. Co-immunoprecipitation was then performed with the protein variants and western blotting was used to detect presence of each protein (McShea, 2011).

## Transfection

Co-transfection was performed to introduce constructs into S3 *Drosophila melanogaster* cells. Since new deletion mutant constructs were not available in time, various *mig-10* and *abi-1* constructs

were co-transfected along with *arm::GAL4* to drive expression. After 3-4 days transfections were checked for GFP expression using a fluorescence microscope. Only the GFP tag is fluorescent, therefore only transfections including *abi-1* constructs with GFP tags were visible. Most transfections showed approximately 5-15% of cells glowing (Figure 15).

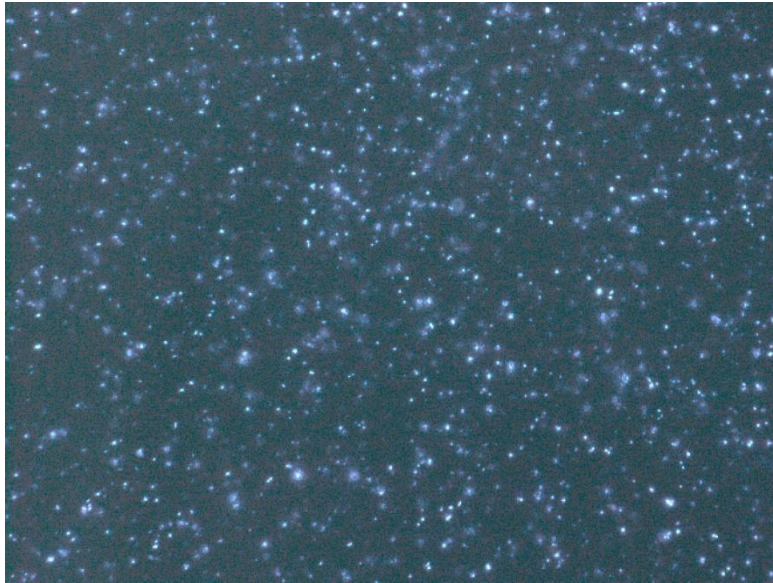


**Figure 15: Co-transfection of *abi-1::GFP*.** Constructs encoding ABI-1 and MIG-10 wild-type and mutant proteins were co-transfected for expression in an insect cell system. Glowing cells indicate cells which are expressing GFP, indicating that ABI-1::GFP protein is being expressed. This picture represents a very efficient co-transfection.

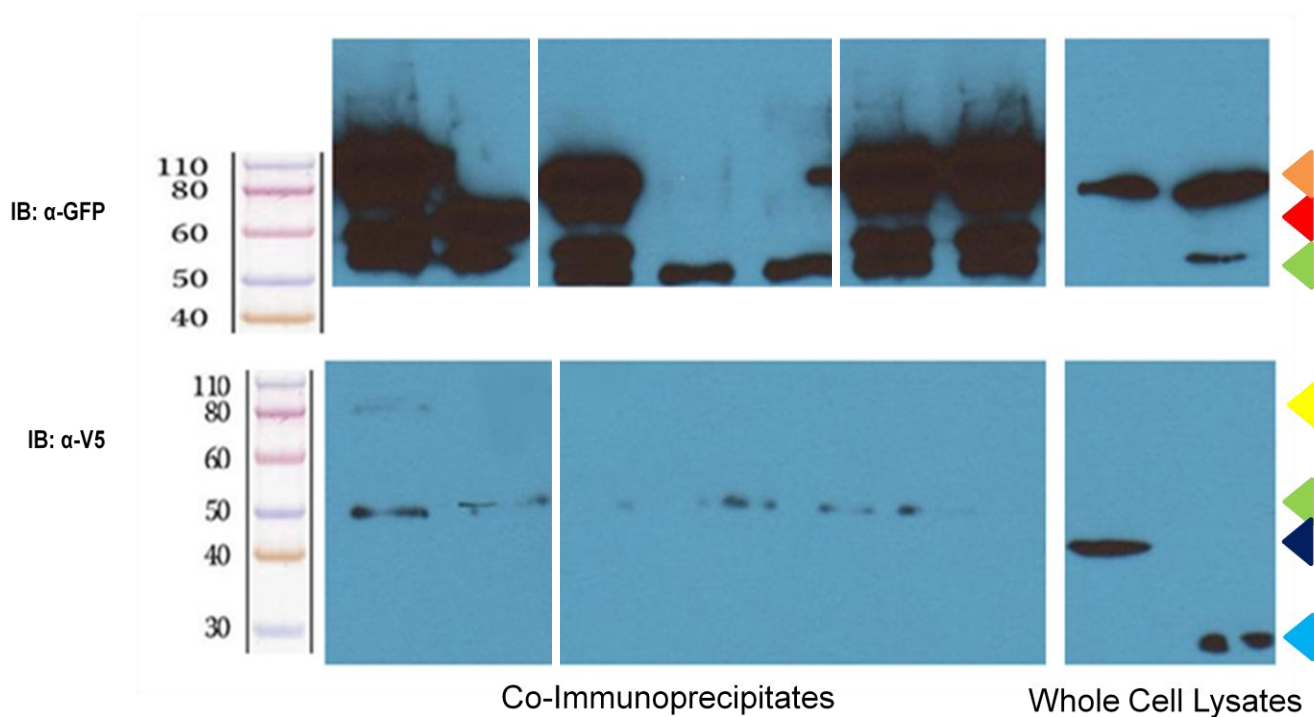
### **Co-Immunoprecipitation and Western Blotting**

Experiments with co-transfected cultures that showed >5% glowing cells were then harvested. 200  $\mu$ L of each well was removed for whole cell lysate samples that did not undergo co-immunoprecipitation and were used as controls on western blots to show presence of proteins in the lysates. Co-immunoprecipitations were then performed on the remainder of the lysates and analyzed by western blotting.

Previously, McShea (2011) found that two regions of MIG-10, the RAPH region and the C-terminus, may interact with ABI-1. In order to confirm which regions of MIG-10 interact with ABI-1, MIG-10 variants MIG-10(RAPH)::V5 and MIG-10(C-term)::V5 were co-immunoprecipitated with wild-type ABI-1::GFP. In addition, ABI-1::GFP and MIG-10A::V5 were co-immunoprecipitated as a positive control and ABI-1(174-426)::GFP and MIG-10A::V5 were co-immunoprecipitated as a negative control. ABI-1::GFP and MIG-10 variants were also co-immunoprecipitated singly to control for specificity of the co-immunoprecipitation assay. ABI-1 variants tagged with GFP were pulled down by anti-GFP antibody during co-immunoprecipitation. Co-immunoprecipitates probed with mouse monoclonal anti-GFP antibody show ABI-1 variants that were pulled down with anti-GFP antibody, visible in Figure 16 (IB:  $\alpha$ -GFP) below. Background bands in co-immunoprecipitation lanes of each experiment are seen at about 50 kDa and are likely due to the magnetic Protein A Sepharose beads used in the co-immunoprecipitation assay. Wild-type ABI-1::GFP is visible at approximately 80 kDa in lanes 1, 3, 6 and 7, indicating that all ABI-1::GFP lysates were pulled down with anti-GFP antibody. ABI-1::GFP is also seen at 80 kDa in the whole cell lysates of the experimental co-transfections (lanes 8 and 9). ABI-1(174-426)::GFP is visible at approximately 56 kDa and in lane 2.

The same co-immunoprecipitates were blotted and probed for V5 (Figure 16; IB:  $\alpha$ -V5). Wild-type MIG-10A::V5 is faintly visible at approximately 79 kDa in the positive control lane 1, indicating that MIG-10A::V5 did interact with ABI-1::GFP. MIG-10A::V5 is not visible in the negative control (lane 2). MIG-10(RAPH)::V5 is visible at approximately 44 kDa in whole cell lysate lane 8 and MIG-10(C-term)::V5 is visible at approximately 23 kDa in whole cell lysate lane 9. However, neither MIG-10(RAPH)::V5 or MIG-10(C-term)::V5 is visible in the experimental co-immunoprecipitation lanes (lanes 6 and 7 respectively), indicating that neither MIG-10 variant had strong interaction with ABI-1::GFP. These data contradict previous results. Though control data was weak, these data suggest that neither the RAPH region nor the C-terminus of MIG-10 is sufficient for interaction with ABI-1.

MIG-10A::V5	+	+							
ABI-1::GFP	+		+			+	+	+	+
ABI-1 (174-426)::GFP		+							
MIG-10 (RAPH)::V5				+		+		+	
MIG-10 (C-term)::V5					+		+		+
Lane	1	2	3	4	5	6	7	8	9



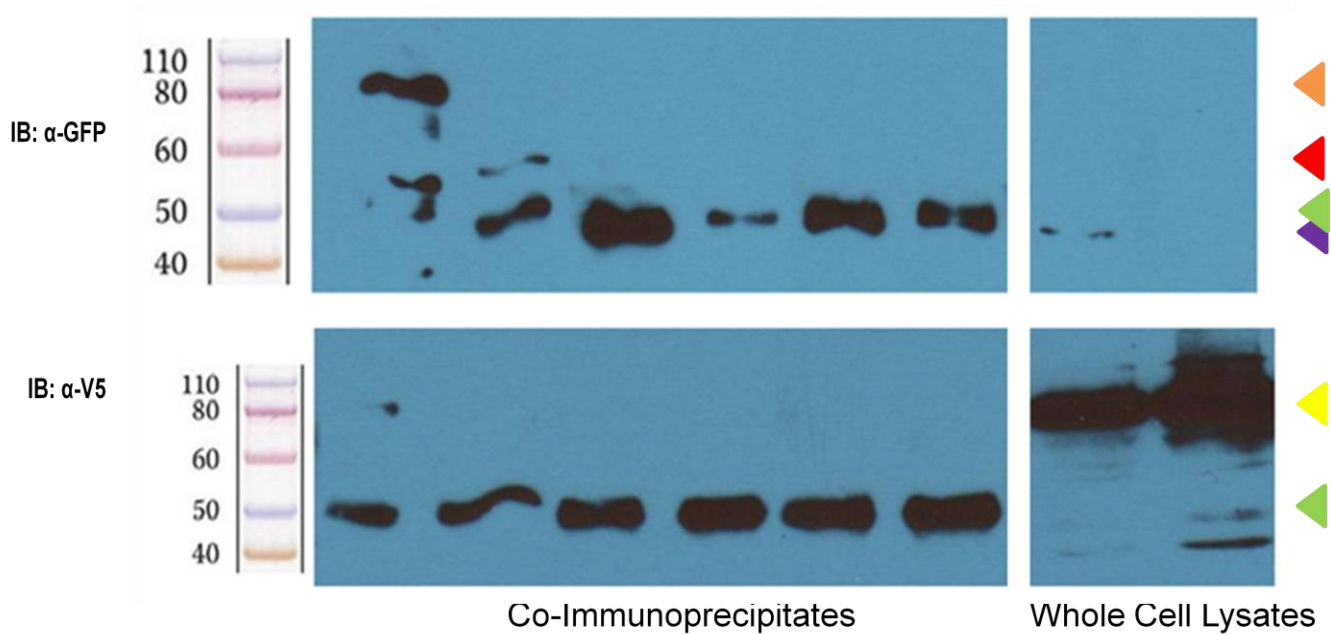
### Legend

MIG-10A::V5	◀	MIG-10(C-term)::V5	◀	MIG-10(RAPH)::V5	◀
ABI-1::GFP	◀	ABI-1(174-426)::GFP	◀	Co-IP Background	◀

**Figure 16: Western Blot of Mig-10 Variants Pulled Down With  $\alpha$ -GFP and Probed for GFP and V5.** Insect cells were co-transfected with *mig-10* and *abi-1* constructs as shown in the table. Cells were immunoprecipitated with  $\alpha$ -GFP antibody and probed with  $\alpha$ -GFP antibody (upper blot) or  $\alpha$ -V5 antibody (lower blot). Whole cell lysates were run for each experimental well (right end of each blot). MIG-10 and ABI-1 variants are indicated by the colored arrows in the legend.

Previous preliminary results suggest that either the N-terminus or the C-terminal SH3 region of ABI-1 may be required for interaction with MIG-10 (McShea, 2011). In order to determine if the N-terminus of ABI-1 interacts with MIG-10, ABI-1 variant ABI-1(1-173)::GFP was co-immunoprecipitated with wild-type MIG-10A::V5. ABI-1 variants tagged with GFP were pulled down by anti-GFP antibody during co-immunoprecipitation and probed with mouse monoclonal anti-GFP antibody (Figure 17; IB:  $\alpha$ -GFP). ABI-1::GFP is visible in lane 1 (80 kDa) and ABI-1(174-426)::GFP is visible in lane 2 (56 kDa). The N-terminus, ABI-1(1-173)::GFP, is 48 kDa and appears as a doublet with the 50 kDa background in lanes 3, 5 and 6 and is visible in whole cell lysate lane 7 (corresponding to the lane 5 sample). ABI-1(1-173)::GFP is not seen in whole cell lysate lane 8 (corresponding to the lane 6 sample), however it appears the protein was present in the co-immunoprecipitate sample, as the band appears thicker and doublet-like compared to lanes with no ABI-1(1-173)::GFP, such as lane 4. The same co-immunoprecipitates were blotted and probed for V5 (Figure 17; IB:  $\alpha$ -V5). MIG-10A::V5 is seen at 79 kDa in the positive control lane 1 and in whole cell lysate samples, lanes 7 and 8. MIG-10A::V5 is not visible in the negative control lane as expected and is also not visible in any of the experimental lanes (5 and 6) also containing ABI-1(1-173)::GFP. These data are consistent with previous results and indicate that the N-terminal region of ABI-1 did not have strong interaction with MIG-10A.

MIG-10A::V5	+	+		+	+	+	+	+
ABI-1::GFP	+							
ABI-1 (174-426)::GFP		+						
ABI-1 (1-173)::GFP			+		+	+	+	+
Lane	1	2	3	4	5	6	7	8



**Legend**

MIG-10A::V5 ▶ ABI-1(1-173)::GFP ▶  
 ABI-1::GFP ▶ ABI-1(174-426)::GFP ▶ Co-IP Background ▶

**Figure 17: Western Blot of ABI-1(1-173)::GFP Pulled Down With  $\alpha$ -GFP and Probed for GFP and V5.** Insect cells were co-transfected with *mig-10* and *abi-1* constructs as shown in the table. Cells were immunoprecipitated with  $\alpha$ -GFP antibody and probed with  $\alpha$ -GFP antibody (upper blot) or  $\alpha$ -V5 antibody (lower blot). Whole cell lysates were run for each experimental well (right end of each blot). MIG-10 and ABI-1 variants are indicated by the colored arrows in the legend.

## Discussion

This project set out to determine the domains required for interaction between MIG-10 and ABI-1, two proteins important in neuronal migration and outgrowth. Results from this project suggest that MIG-10(RAPH)::V5 and MIG-10(C-term)::V5 may not be sufficient for interaction with ABI-1::GFP (Figure 16). These data contradict previous results in which MIG-10(RAPH)::V5 and MIG-10(C-term)::V5 each showed some interaction with ABI-1::GFP and ABI-1(426-469)::GFP (McShea, 2011). The RAPH region and C-terminus of MIG-10 both contain SH3 binding sites, making both regions logical candidates for interaction with the C-terminal SH3 binding site of ABI-1. New data from this project should not be used to make a conclusion about possible interaction of MIG-10 variants and ABI-1 because the positive control band was weak. It is possible that there was some interaction between the MIG-10 variants and ABI-1 which was not seen on the western blot due to weaker signals than the positive control. Ultimately, this experiment should be repeated for more concrete results.

In addition, results from this project indicate that the N terminus of ABI-1, ABI-1(1-173)::GFP, containing WAB, Q-SNARE and ABL-HHR domains, is not sufficient for interaction with MIG-10A::V5 (Figure 17). Although these results also contain a relatively weak positive control band, these data support previous research which suggested that ABI-1(1-173)::GFP was not sufficient for interaction with MIG-10A::V5 (McShea, 2011). Thus, previous and current data are consistent with the hypothesis that the N-terminus of ABI-1 is not sufficient for interaction with MIG-10. McShea had also previously determined that the middle domain of ABI-1, ABI-1(174-426)::GFP, containing serine rich regions and SH3 binding sites, was not sufficient for interaction with MIG-10A::V5. Data from McShea's experiments suggest that the C-terminal SH3 domain of ABI-1 is required for interaction with MIG-10, and may interact with several domains of MIG-10 such as the RAPH and C-terminal regions. This hypothesis is logical biochemically because MIG-10 contains thirteen SH3 binding sites, across several domains of the

protein, each of which could potentially bind the SH3 region of ABI-1. However, this project was not specifically able to test this hypothesis due to time constraints.

This project prepared new deletion mutant constructs in order to determine if the SH3 domain of ABI-1 is necessary and sufficient for MIG-10. Constructs, *abi-1(1-415)::GFP* and *abi-1(1-426)::GFP*, each missing a portion or the entire SH3 domain, were created to test the first half of the hypothesis. Constructs were not confirmed in time for use in this project; however, future co-immunoprecipitation experiments should be conducted with these new constructs to determine if the SH3 domain is necessary for interaction with MIG-10A::V5. A negative result, meaning a lack of binding between both constructs and MIG-10 would support the hypothesis that the SH3 domain of ABI-1 is required for interaction with MIG-10. The third new deletion mutant construct, *abi-1(416-469)::GFP*, containing only the C-terminal SH3 domain, was created to determine if the SH3 domain is sufficient for interaction with MIG-10A::V5. A positive result would support the hypothesis that the SH3 domain of ABI-1 is sufficient for interaction with MIG-10.

When conducting future experiments, several technical aspects of assays used during this project should be considered. First, any additional cloning experiments should consider the age of *E. coli* cells, as older cells likely caused a great decrease in the efficiency of cloning during these experiments. Second, the health of the *D. melanogaster* S3 cells could affect transfection efficiency. During this project, cells were extending processes and dividing less frequently than normal which could possibly affect the uptake of desired genes into the cells during transfection. Future experiments may need to manipulate cell culture techniques (such as using conditioned media) to maintain a healthier cell culture. Next, co-immunoprecipitation and western assays could be manipulated for stronger results by trying different lysis buffers, storage time and temperatures (-20°C or 4°C) of co-immunoprecipitate samples, and film exposure levels. For example, buffers should be manipulated because buffers that are too

stringent may interrupt protein-protein interactions and cause a false result which can be interpreted as lack of interaction. If time and resources permit, whole cell lysates should also be performed on all MIG-10 variants in an experiment, to confirm presence of MIG-10 variants in cases where no binding is seen, i.e. negative controls and negative experimental results.

One pitfall of using deletion mutant proteins to determine the domains involved in interaction is the possibility of deleterious effects on protein folding. When a gene is manipulated, such as removing portions of the gene, it can result in an unstable protein or impact the folding of the overall protein. Protein shape is crucial for interaction with other proteins. If a protein folds differently due to deletion mutations, this may cause lack of interaction where interaction should occur and result in incorrect conclusions. Whole cell lysates can also be used to determine if there are severe differences in folding. If a protein does not run as expected on a gel, it is possible that the protein shape has been significantly altered. In the future, if altered protein-shape or instability appears to be impacting protein-protein interactions, then other types of mutations, particularly more targeted ones such as point mutations, should be considered. A useful way to use point mutation would be to find an amino acid likely to be involved in the wild-type interaction and change the amino acid such that it may no longer interact with the other protein, without altering the protein shape.

Once the domains required for *in vitro* interaction between MIG-10 and ABI-1 have been identified, further work should be done to determine the implications of this interaction *in vivo*. For example, it is not currently clear where *abi-1* fits in the axonal outgrowth signal transduction pathway. Genetic analysis should be done to determine where *abi-1* fits into the order of the pathway and what may occur downstream of *abi-1*. The axon guidance pathway may also involve other proteins in addition to ABI-1, as interaction with ABI-1 in vertebrates is known to lead to phosphorylation and activation of other proteins such as Mena, Rac, and WAVE. Once more is known about the *C. elegans* neuronal

migration and axon guidance pathways, scientists can use this information to help strengthen their understanding of how MIG-10 orthologs, Lamellipodin and RIAM, and vertebrate ABI proteins may interact in vertebrate neuronal migration and axon guidance pathways. Ultimately, this research will increase understanding of neuronal migration and axon guidance pathways in humans , which will in turn contribute to creation of neuroregenerative therapies to alleviate symptoms of neuronal migration disorders.

## References

- Adler, C.E., Fetter, R.D., and Bargmann, C.I. (2006). UNC-6/Netrin induces neuronal asymmetry and defines the site of axon formation. *Nat Neurosci* **9**:511-518.
- Bear, M. F., Connors, B. W., and Paradiso, M. A. (2007). *Neuroscience: Exploring the Brain*. 3<sup>rd</sup> Edition. Philadelphia: Lippincott Williams and Wilkins.
- Brenner, S. (1974). The genetics of *Caenorhabditis elegans*. *Genetics* **77**: 71-94.
- Buechner, M. (2002). Tubes and the single *C. elegans* excretory cell. *Trends Cell Biol* **12**: 479-484.
- Chalfie, M., Tu, Y., Euskirchen, G., Ward, W.W., and Prasher, D.C. (1994). Green fluorescent protein as a marker for gene expression. *Science* **263**:802-805.
- Chang, C., Adler, C.E., Krause, M., Clark, S.G., Gertler, F.B., Tessier-Lavigne, M., and Bargmann, C.I. (2006). MIG-10/Lamellipodin and AGE-1/PI3K promote axon guidance and outgrowth in response to Slit and Netrin. *Curr Biol* **16**:854-862.
- Disanza, A., Steffen, A., Hertzog, M., Frittoli, E., Rottner, K., and Scita, G. (2005). Actin polymerization machinery: the finish line of signaling networks, the starting point of cellular movement. *Cell. Mol. Life Sci.* **62**: 955-970.
- Dubuke, M. and Grant, C. (2009). ABI-1 interacts with MIG-10: protein interaction in neuronal migration in *Caenorhabditis elegans*. Senior Undergraduate MQP. Worcester, MA: Worcester Polytechnic Institute.
- Echarri, A., Lai, M.J., Robinson, M.R., and Pendergast, A.M. (2004). Abl Interactor 1 (Abi-1) Wave-binding and SNARE domains regulate its nucleocytoplasmic shuttling, lamellipodium localization, and Wave-1 levels. *Mol Cell Biol* **24**:4979-4993.
- Engle, E.C. (2010). Human genetic disorders of axon guidance. *Cold Spring Harb Perspect Biol.* **2**: a001784.
- Gosselin, J. and O'Toole, S. (2008). MIG-10, an adaptor protein, interacts with ABI-1, a component of actin polymerization machinery. Senior Undergraduate MQP. Worcester, MA: Worcester Polytechnic Institute.
- Hedgecock, E.M., Culotti, J.G., Hall, D.H., and Stern, B.D. (1987). Genetics of cell and axon migrations in *Caenorhabditis elegans*. *Development* **100**: 365-382.
- Krause, M., Leslie, J.D., Stewart, M., Lafuente, E.M., Valderrama, F., Jagannathan, R., Strasser, G.A., Rubinson, D.A., Liu, H., Way, M., Yaffe, M.B., Boussiotis, V.A., and Gertler, F.B. (2004). Lamellipodin, an Ena/VASP ligand, is implicated in the regulation of lamellipodial dynamics. *Dev Cell* **7**:571-583.

- Lafuente, E.M., van Puijenbroek, A.A., Krause, M., Carman, C.V., Freeman, G.J., Berezovskaya, A., Constantine, E., Springer, T.A., Gertler, F.B., and Boussiotis, V.A. (2004). RIAM, an Ena/VASP and Profilin ligand, interacts with Rap1-GTP and mediates Rap1-induced adhesion. *Dev Cell* **7**:585-595.
- Manser, J. and Wood, W.B. (1990). Mutations affecting embryonic cell migrations in *Caenorhabditis elegans*. *Dev Gen* **11**: 49-64.
- Manser, J., Roonprapunt, C., and Margolis, B. (1997). *C. elegans* cell migration gene *mig-10* shares similarities with a family of SH2 domain proteins and acts cell nonautonomously in excretory canal development. *Dev Biol* **184**: 150-164.
- McShea, M. (2011). Evidence of an interaction between the actin cytoskeletal regulators MIG-10 and ABI-1. Master's Thesis. Worcester, MA: Worcester Polytechnic Institute.
- Michael, M., Vehlow, A., Navarro, C., and Krause, M. (2010). c-Abl, Lamellipodin, and Ena/VASP proteins cooperate in dorsal ruffling of fibroblasts and axonal morphogenesis. *Curr Biol* **20**:783-791.
- Schmidt, K.L., Marcus-Gueret, N., Adeleye, A., Webber, J., Baillie, D., and Stringham, E.G. (2009). The cell migration molecule UNC-53/NAV2 is linked to the ARP2/3 complex by ABI-1. *Development* **136**:563-574.
- Tani, K., Sato, S., Sukezane, T., Kojima, H., Hirose, H., Hanafusa, H., and Shishido, T. (2003). Abl Interactor 1 promotes tyrosine 296 phosphorylation of mammalian Enabled (Mena) by c-Abl kinase. *J Biol Chem* **278**:21685-21692.
- Quinn, C.C., Pfeil, D.S., and Wadsworth, W.G. (2008). CED-10/Rac1 mediates axon guidance by regulating the asymmetric distribution of MIG-10/Lamellipodin. *Curr Biol* **18**:808-813.
- Quinn, C.C., Pfeil, D.S., Chen, E., Stovall, E.L., Harden, M.V., Gavin, M.K., Forrester, W.C., Ryder, E.F., Soto, M.C., and Wadsworth, W.G. (2006). UNC-6/Netrin and SLT-1/Slit guidance cues orient axon outgrowth mediated by MIG-10/RIAM/Lamellipodin. *Curr Biol* **16**:845-853.
- Quinn, C.C. and Wadsworth, W.G (2008). Axon guidance: asymmetric signaling orients polarized outgrowth. *Trends in Cell Biology* **18**: 597-603.
- Wormbase. Retrieved February 16, 2012 from <http://wormbase.org/db/gene/gene?name=WBGene00003243;class=Gene>.
- Zhang, Subaiou. (2010). Functional analysis of MIG-10: a cytoplasmic adaptor protein important in neuronal migration and process outgrowth in *C. elegans*. Senior Undergraduate MQP. Worcester, MA: Worcester Polytechnic Institute.